Available online at www.sciencedirect.com
ScienceDirect
Nuclear Physics A 00 (2020) 1–4
Nuclear Physics A
www.elsevier.com/locate/procedia

XXVIIIth International Conference on Ultrarelativistic Nucleus-Nucleus Collisions
(Quark Matter 2019)

Measurement of cumulants of conserved charge multiplicity distributions in Au+Au collisions from the STAR experiment

Ashish Pandav for the STAR Collaboration

School of Physical Sciences, National Institute of Science Education and Research, HBNI, Jatni-752050, INDIA

Abstract

We report on collision-centrality dependence of cumulants of event-by-event net-proton and net-charge distributions in Au+Au collisions for center-of-mass energy of $\sqrt{s_{NN}}$ = 54.4 GeV from the STAR experiment. Strong collision-centrality dependence is observed for cumulants ($C_n, n \leq 4$) of the net-proton and net-charge distributions. The cumulant ratios C_3/C_2, C_4/C_2, and C_6/C_2 exhibit a weak collision-centrality dependence. The C_6/C_2 of net-proton and net-charge distributions for most central gold nuclei collisions at $\sqrt{s_{NN}}$ = 54.4 GeV show positive sign while it remains negative for net-proton distribution at $\sqrt{s_{NN}}$ = 200 GeV for the same collision system and centrality. To understand effects of acceptance and baryon number conservation, the measurements are compared to expectations from the UrQMD and HIJING models calculated within the STAR detector acceptance.

Keywords: QCD phase diagram, QCD critical point, conserved charge fluctuations, cumulants

1. Introduction

One of the major goals of heavy-ion collision experiments is to explore the Quantum Chromodynamics (QCD) phase diagram and search for the QCD critical point. Lattice QCD calculations have shown that for vanishing baryonic chemical potential (μ_B), the nature of phase transition between quark-gluon plasma (QGP) and hadronic matter is a smooth crossover [1] whereas QCD-based models suggest this phase transition to be of first order for finite μ_B [2]. The cumulants of conserved quantities in strong interactions are proposed to be sensitive observables for the search of the QCD critical point and the phase transition between quark-gluon plasma (QGP) and hadronic matter [3]. The cumulants and their ratios are related to the correlation length of the hot and dense medium formed in the heavy ion collisions and the thermodynamic susceptibilities that are calculable via various QCD-based models and lattice QCD [4, 5].

Cumulants quantify the traits of a distribution, for example, the first- and second-order cumulant (C_1 and C_2) are the mean and variance of a distribution whereas the third- and fourth-order cumulants (C_3 and C_4) encode the skewness and kurtosis of a distribution, respectively. Cumulants and their ratios for event-by-event distributions of net-charge, net-kaon, and net-proton in collisions of gold nuclei were measured by the STAR detector in the phase I of Beam Energy Scan (BES) program at the Relativistic Heavy Ion Collider

(RHIC) [6–10]. Theoretical calculations show that the net-proton number fluctuations could reliably reflect the baryon number susceptibility at the critical point [11]. Non-monotonic dependence on beam energy is observed for the cumulant ratios C_3/C_2 and C_4/C_2 of net-proton distribution in the most central (0-5%) collisions, which may hint at existence of a possible critical point. The sixth-order cumulants (C_6) provides insights into the nature of phase transition. Negative C_6/C_2 of net-baryon and net-charge distributions are predicted from a QCD-based model for crossover phase transitions, if the chemical freeze-out is close to the chiral phase transition [12–14].

2. Analysis techniques

About ~ 550 million events are analysed for obtaining cumulants of net-particle distributions in Au+Au collisions at $\sqrt{s_{NN}}$ = 54.4 GeV. Time Projection Chamber (TPC) and Time-of-Flight (TOF) detectors [15] are used to select protons (antiprotons) within p_T range 0.4 – 2.0 GeV/c, and charged pions and kaons within p_T range 0.2 – 1.6 GeV/c. The rapidity coverage $|y| < 0.5$ is used to select charged particles for measuring net-proton while psuedorapidity coverage $|\eta| < 0.5$ is considered for charged particle selection for net-charge fluctuation measurements. The collision centrality is determined from the charged particle multiplicity excluding the particles of interest to avoid the autocorrelation effect [16]. In order to suppress the volume fluctuation effects, centrality bin width correction is applied to the measurement of the cumulants [17–19]. Cumulants are corrected for acceptance and detection inefficiencies, with the assumption that the distribution of the detector response is binomial [20, 21]. For estimation of statistical uncertainties of cumulants and their ratios, Delta theorem method and a resampling method called the Bootstrap are used [22, 23]. Systematic uncertainties of the C_n's are estimated varying tracking efficiency, track selection and particle identification criteria.

3. Results

3.1. Cumulants of net-particle distributions

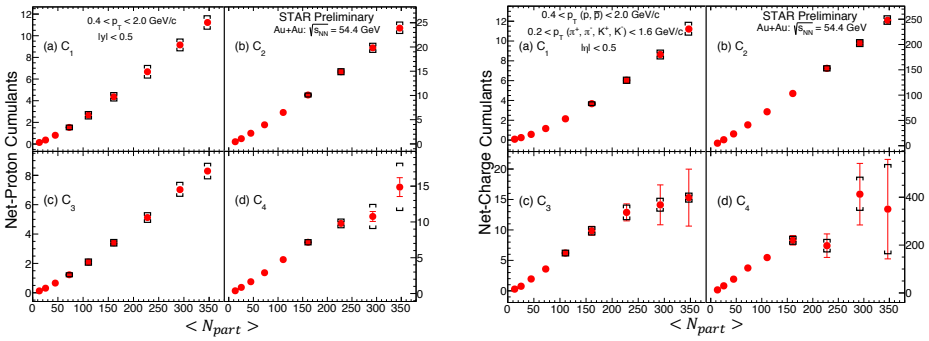

Fig. 1. Cumulants ($C_n, n \leq 4$) of net-proton and net-charge distributions as a function of average number of participant nucleons for Au+Au collisions at $\sqrt{s_{NN}}$ = 54.4 GeV.

Cumulants up to the 4^{th} order of the event-by-event net-proton and net-charge distributions for Au+Au collisions at $\sqrt{s_{NN}}$ = 54.4 GeV as a function of collision centrality (given by the average number of participant nucleons, <Npart>) are presented in Fig. 1. The statistical and systematic uncertainties on the measurements are shown by red bars and black brackets, respectively. Cumulants of the net-proton and net-charge distributions increase from peripheral to central collisions. Cumulants of the net-charge distribution have larger statistical uncertainties for a given centrality which can be attributed to the larger width of net-charge distributions as compared to net-proton distributions.

3.2. Cumulant ratios of net-proton and net-charge distributions

Figure 2, panel (a) and (b), shows collision-centrality dependence of cumulant ratios C_3/C_2 and C_4/C_2 ($S\sigma$ and $\kappa\sigma^2$ respectively) of net-proton and net-charge distributions constructed from the measured cumulant values. The cumulant ratios C_3/C_2 and C_4/C_2 exhibit a weak dependence on collision centrality for net-proton and net-charge distributions. The expectations from the UrQMD and HIJING models are also compared to the measurements [24, 25]. The model expectations are inconsistent with the measurements and only qualitatively reproduce the measured centrality dependence of the cumulant ratios. The Skellam baseline for C_3/C_2 and C_4/C_2 of net-proton and net-charge distributions, which is the expected values of the ratios under the assumption that protons (positively charged particles) and antiprotons (negatively charged particles) follow independent Poisson distributions, fails to describe the measured values. Beam-energy dependence of the cumulant ratio C_4/C_2 of net-proton and net-charge distributions for peripheral (70-80%) and most central (0-5%) collisions, including the results from the current measurement (open and solid red markers respectively) are shown in the panel (c) and (d) of Fig 2. Non-monotonic beam energy dependence of C_4/C_2 is observed for net-proton distribution while C_4/C_2 of net-charge distributions show monotonic variation as a function of beam energy. The new C_4/C_2 measurements at $\sqrt{s_{NN}}$ = 54.4 GeV are consistent with the trends established for the other BES energies.

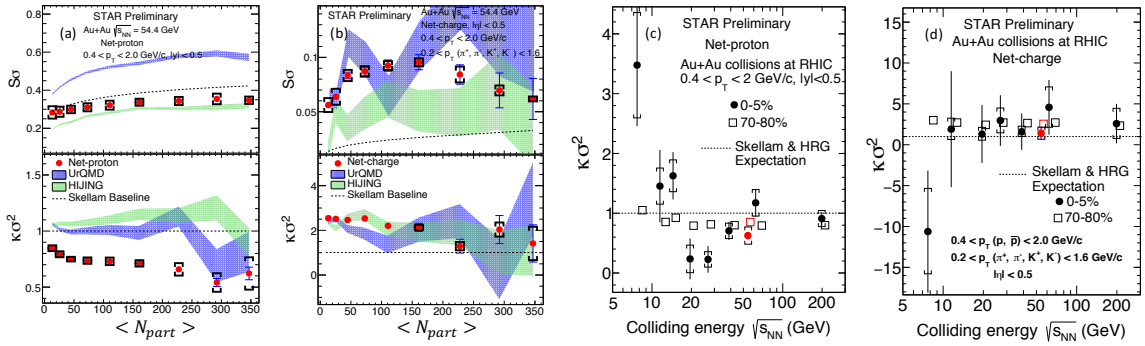

Fig. 2. Panel a and b shows cumulant ratios C_3/C_2 and C_4/C_2 of net-proton and net-charge distributions as a function of average number of participant nucleons for Au+Au collisions at $\sqrt{s_{NN}}$ = 54.4 GeV. The blue and green band presents the UrQMD and HIJING model expectations caculated in the STAR acceptance, respectively. The Skellam baseline is given by black dotted line. Panel c and d shows beam-energy dependence of C_4/C_2 for net-proton and net-charge distributions for 0-5% and 70-80% most central collisions for Au+Au collisions with inclusion of the results from the C_4/C_2 measurement at $\sqrt{s_{NN}}$ = 54.4 GeV (red markers).

3.3. The sixth-order cumulant

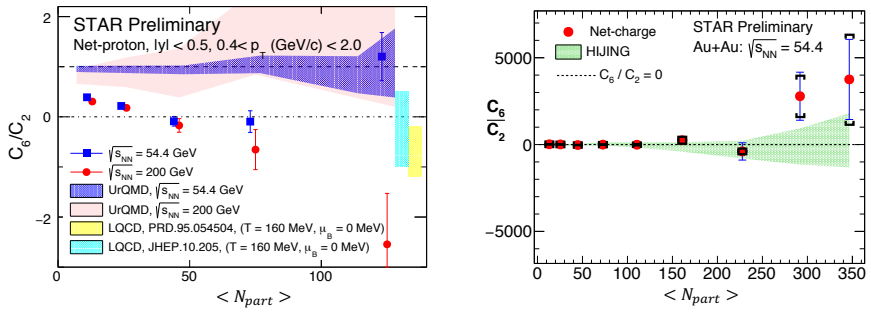

Fig. 3. (Left plot) The C_6/C_2 of net-proton distribution for Au+Au collisions at $\sqrt{s_{NN}}$ = 54.4 GeV (blue) and 200 GeV (red) as a function of collision centrality. Red and blue bands are the UrQMD expectations for Au+Au collisions at $\sqrt{s_{NN}}$ = 200 and 54.4 GeV, respectively. The yellow and turquoise band are the Lattice QCD predictions. (Right plot) The C_6/C_2 of net-charge distribution for Au+Au collisions at $\sqrt{s_{NN}}$ = 54.4 GeV as a function of collision centrality. Green band is the HIJING model expectation.

The collision-centrality dependence of the ratio of the sixth- to second-order cumulants (C_6/C_2) of net-proton and net-charge distributions for Au+Au collisions are shown in Fig 3. The C_6/C_2 of net-proton distributions for central collisions (0-40%) at $\sqrt{s_{NN}}$ = 54.4 GeV is positive while C_6/C_2 measured at $\sqrt{s_{NN}}$ = 200 GeV is negative for the same collision centrality [26]. A negative C_6/C_2 is predicted for the crossover phase transition between hadronic matter and quark-gluon plasma in QCD-based calculations [12]. The UrQMD model expectations for Au+Au collisions at $\sqrt{s_{NN}}$ = 200 GeV and $\sqrt{s_{NN}}$ = 54.4 GeV are found to be positive and consistent with the Skellam baseline across all collision centralities. The C_6/C_2 of net-charge distribution for Au+Au collisions at $\sqrt{s_{NN}}$ = 54.4 GeV for two most central collision classes (0-5% and 5-10%) show positive sign.

4. Summary

We presented the collision-centrality dependence of cumulants and cumulant ratios of net-proton and net-charge distributions from high statistics Au+Au collisions at $\sqrt{s_{NN}}$ = 54.4 GeV. The cumulant ratios C_3/C_2, C_4/C_2 and C_6/C_2 exhibit a weak collision-centrality dependence. The C_4/C_2 ($\kappa\sigma^2$) measurement of net-proton and net-charge distributions at $\sqrt{s_{NN}}$ = 54.4 GeV are consistent with the existing beam energy trend of C_4/C_2 from the BES-I program. Furthurmore, the C_6/C_2 of net-proton distribution for Au+Au collisions at $\sqrt{s_{NN}}$ = 200 GeV for most central collisions (0-40%) is negative, and this could be an experimental evidence of crossover phase transition. Using the Taylor expansion at finite μ_B, lattice QCD calculation predicts the sign of C_6/C_2 of net-baryon at $\sqrt{s_{NN}}$ = 54.4 GeV and 200 GeV to be negative [13, 14]. However, there are limitations in comparing experimental data with lattice QCD calculations as they are calculated for net-proton distributions instead of net-baryon distributions and the experimental measurements are made within specific kinematic range. The new measurements at $\sqrt{s_{NN}}$ = 54.4 GeV serve as precise baselines for the critical fluctuation studies which are expected at lower center-of-mass energies.

5. Acknowledgments

We acknowledge the financial support by Department of Atomic Energy, Govt. of India.

References

[1] Y. Aoki, G. Endrodi, Z. Fodor, S. D. Katz and K. K. Szabo, Nature **443**, 675 (2006).
[2] S. Ejiri, Phys. Rev. **D78**, 074507 (2008).
[3] M. A. Stephanov, Phys. Rev. Lett. **102**, 032301 (2009).
[4] R. V. Gavai and S. Gupta, Phys. Lett. **B696**, 459 (2011).
[5] S. Gupta, X. Luo, B. Mohanty, H. G. Ritter and N. Xu, Science **332**, 1525 (2011).
[6] L. Adamczyk *et al.* [STAR Collaboration], Phys. Rev. Lett. **113**, 092301 (2014).
[7] L. Adamczyk *et al.* [STAR Collaboration], Phys. Lett. **B785**, 551 (2018).
[8] M. M. Aggarwal *et al.* [STAR Collaboration], Phys. Rev. Lett. **105**, 022302 (2010).
[9] L. Adamczyk *et al.* [STAR Collaboration], Phys. Rev. Lett. **112**, 032302 (2014).
[10] J. Adam *et al.*, [STAR Collaboration], arXiv:2001.02852.
[11] Y.Hatta and M. A. Stephanov, Phys. Rev. Lett. **91**, 102003 (2003).
[12] B. Friman *et al.*, Eur. 346 Phys. J. **C71**, 1694 (2011).
[13] A. Bazavov *et al.*, Phys. Rev. **D101** , 074502 (2020) .
[14] H. T. Ding, arXiv:2002.11957.
[15] M. Shao *et al.*, Nucl. Instrum. Meth. **A558**, 419 (2006).
[16] A. Chatterjee, Y. Zhang, J. Zeng, N. R. Sahoo, X. Luo, arXiv:1910.08004.
[17] X. Luo, J. Xu, B. Mohanty and N. Xu, J. Phys. **G40**, 105104 (2013).
[18] P. Braun-Munzinger, A. Rustamov and J. Stachel, Nucl. Phys. **A960** (2019) 114-130.
[19] V. Skokov, B. Friman, and K. Redlich, Phys. Rev. **C88**, 034911 (2013).
[20] X. Luo, Phys. Rev. **C91**, 034907 (2015).
[21] T. Nonaka, M. Kitazawa and S. Esumi, Phys. Rev. **C95**, no. 6, 064912 (2017).
[22] X. Luo, J. Phys. **G39**, 025008 (2012).
[23] A. Pandav, D. Mallick and B. Mohanty, Nucl. Phys. **A991** (2019) 121608.
[24] S. A. Bass *et al.*, Prog. Part. Nucl. Phys. **41**, 255 (1998).
[25] M. Gyulassy *et al.*, Comput. Phys. Commun. **83**, 307 (1994).
[26] T. Nonaka, [STAR collaboration], arXiv:2002.12505 .